An assessment of the quality of microanalysis of silicate glass using scanning electron microscope-based energy dispersive spectrometry (SEM-EDS)

Guilherme A. R. Gualda, Vanderbilt University, Nashville, TN, USA

Alessandro Frontoni, Università Roma Tre, Rome, Italy

Blake M. Wallrich, Corning Inc., Corning, NY, USA

Lydia J. Harmon, Occidental College, Los Angeles, CA, USA

Sarah L. Smithies, University of Canterbury, Christchurch, New Zealand

Genna R. Chiaro, United States Geological Survey, Moffett Field, CA, USA

Ayla S. Pamukçu, Stanford University, Stanford, CA, USA

Revised manuscript submitted to

American Mineralogist

Abstract

The composition of volcanic glass records important clues into the origin and evolution of magmatic systems. However, the analysis of volcanic glass presents challenges when performed using electron-beam techniques, particularly due to Na mobility. While microanalysis of geological materials is usually performed using electron microprobe-based wavelength-dispersive spectrometry (EMP-WDS), we present here results of glass analysis using energy-dispersive spectrometry with a scanning electron microscope (SEM- EDS). We use three U.S. Geological Survey (USGS) whole-rock reference materials (i.e., RGM-1, STM-1, QLO-1) that were fused into glass using a double-fusion technique. Results for 12 sessions over two months using the SEM-EDS reveal excellent reproducibility, agreement with the expected values for RGM-1 and STM-1, and excellent counting statistics when using live acquisition times of 15 s; results for QLO-1 suggest that the fused material is somewhat inhomogeneous. For longer acquisition times (30, 60, 90 s), significant Na migration is observed; we conclude that minimal Na migration takes place with acquisition times of 15 s using our analytical instrumentation. We also compile data for RGM-1 obtained using the same instrument over the last decade, and we further demonstrate the reliability of SEM-EDS for microanalysis of silicate glasses. Comparison of our results with EMP-WDS results for a range of reference materials published by researchers at the USGS Alaska Volcano Observatory suggest that both EMP-WDS and SEM-EDS can yield adequate analysis of volcanic glass, but SEM-EDS can potentially lead to higher precision for major elements (1 wt.% concentration), while EMP-WDS typically leads to higher precision for minor elements. The higher precision of SEM-EDS results for major elements, combined with the more widespread distribution, lower usage cost, and higher ease of use of

such systems, makes analysis via SEM-EDS an attractive option for measuring major-element compositions of volcanic glass.

Paper highlight information

Analysis of volcanic glass is important in petrological studies, but it is also challenging from an analytical standpoint. While analysis is usually performed using the electron microprobe, cost of usage, the complexity of analytical protocols, and the relatively long acquisition times pose challenges to systematic studies of volcanic glass. With the advent of silicon drift detectors (SDD), analysis of Earth materials with energy dispersive spectrometry on a scanning electron microscope (SEM-EDS) presents an attractive alternative to the electron microprobe, providing faster, cheaper, and easier analysis. Yet, there is a need for systematic studies that assess the quality of analysis of volcanic glass using SEM-EDS. We present here a systematic study of three USGS reference materials that we fused into glass using a double-fusion technique. We present the results of a short-term study using all three materials, as well as selected data for reference material RGM-1 collected over the last decade in our laboratory. We also compare our SEM-EDS results with results from a recent study in which a large compilation of electron microprobe data from the USGS Alaska Volcano Observatory is presented. We show that SEM-EDS results have adequate precision, accuracy, and reproducibility, both in the short-term and long-term studies. In fact, we argue that results for major elements are potentially more precise than what is generally obtained using the electron microprobe.

Keywords

volcanic glass; electron-based microanalysis; energy-dispersive spectrometry; scanning electron microscope; wavelength-dispersive spectrometry; electron microprobe

Introduction

Volcanic glass can record important clues into the origin of volcanic rocks and the evolution of magmatic systems. Yet, measuring accurate volcanic glass compositions is often challenging using electron-beam microanalytical techniques due to beam damage during analysis, particularly for glass that is rich in Na and H_2O (e.g., Devine et al. 1995; Morgan and London 2005; Roman et al. 2006; among many others).

Major and minor-element microanalysis of geological materials is traditionally performed using electron microprobe-based wavelength dispersive spectrometry (EMP-WDS), which generally allows for quantification of elements in concentrations of hundreds of parts per million to tens of weight percent (e.g., Potts 1987; Reed 2005). However, due to the geometry and characteristics of WDS spectrometers, each individual EMP-WDS analysis typically takes tens to hundreds of seconds, leading to significant beam damage for beam-sensitive materials such as volcanic glass. Further, EMP-WDS employs relatively high beam currents (when compared to other electron-beam instruments), often as high as several µA, which further contributes to significant beam damage and Na migration when using EMP-WDS. Finally, the combination of relatively high cost of operation, more limited availability of EMP instrumentation, and relatively long analytical times (typically on the order of minutes) often makes it impractical to obtain large numbers of analyses per sample using EMP-WDS, which can be necessary to identify alteration and compositional heterogeneity in natural volcanic glass.

With the advent of solid-state Silicon drift detectors (SDD), the quality of scanning electron microscope-based energy dispersive spectrometry (SEM-EDS) analysis has improved

considerably. Ritchie et al. (2012) show that SEM-EDS analysis of glasses using SDD rivals the precision obtained with EMP-WDS for major (>0.1%) and minor (>0.01%) elements (see also Reed and Ware 1973; Newbury and Ritchie 2015). Further, individual SEM-EDS analyses are obtained much more quickly (~30 s) because all elements are measured simultaneously by a single detector. Finally, incident currents in SEM-EDS analysis are typically on the order of a few nA, up to 3 orders of magnitude lower than what is used in EMP-WDS analysis. Short analytical times, combined with lower incident currents, result in less beam-damage to the analyzed glass. Additionally, the much more widespread availability of SEM and the lower operating costs make it possible to obtain large numbers of glass SEM-EDS analyses quickly and affordably, allowing better characterization of compositional heterogeneity of volcanic glass.

One of the challenges to testing the quality of volcanic glass analyses is finding suitable reference materials that are homogenous and have a well characterized compositions that are similar to natural compositions. In this work, we analyze glasses that we synthesized in the laboratory from powdered U.S. Geological Survey (USGS) whole-rock reference materials – whose compositions are well characterized by independent methods – to assess the quality of SEM-EDS analysis of volcanic glass. We compare data obtained for three different glasses over 12 analytical sessions spanning a short period of time (~2 months). We also present and discuss analytical data for one of these glasses obtained over the last decade on the same instrument at Vanderbilt University.

Materials and Methods

Materials

USGS whole-rock powder reference materials RGM-1, STM-1, and QLO-1 were used in this study (Flanagan 1976; Abbey 1983; Gladney and Roelandts 1988; Govindaraju 1994). RGM-1 corresponds to a rhyolite, STM-1 is a nepheline syenite, and QLO-1 is a quartz latite. Together, these three reference materials span a wide range of compositions representative of silicic magmas (Table 1).

Powders were synthesized into glass using a double-fusion technique, to ensure complete homogenization and melting of the starting powders, under atmospheric pressure in a Thermolyne 46100 benchtop muffle high-temperature furnace. Powders were transferred into a Platinum crucible with a tight-fitting lid and placed in a preheated furnace at temperatures of 1000 °C for 1 hour, to limit volatilization of Na. Temperatures were then increased to 1600 °C and held for two hours. Following the hold at 1600 °C, the crucibles were extracted from the furnace and quenched in a bucket of ice water.

Glass beads retrieved after fusion were mounted in epoxy mounts, ground to expose bead surfaces large enough for analysis (typically ~1 mm across) and polished to 0.5 µm grit. Mounts were carbon-coated prior to analysis.

Analytical method

SEM-EDS analysis was performed using an Oxford AZtecEnergy Advanced Microanalysis System equipped with an X-Max 50 mm^2 large-area Energy Dispersive SDD attached to a Tescan Vega3

Variable-Pressure SEM installed in the Department of Earth & Environmental Sciences at Vanderbilt University (EES-Vanderbilt). Analysis was performed using standard protocols employed in prior work focusing on volcanic glass at EES-Vanderbilt (Gualda et al. 2018, 2022; Pamukçu et al. 2020; Pitcher et al. 2021; Smithies et al. 2023; Chiaro et al. 2024; Harmon et al. 2024a, 2024b), which consist of:

- Accelerating voltage of 15 kV.
- Working distance of 15 mm, which is the optimized working distance for EDS analysis in the EES-Vanderbilt system.
- Beam intensity set to 17-20, yielding absorbed currents of ~2-5 nA.
- Analysis areas as rectangles of variable sizes, but with typical height and width of 10-50 µm (Figure 1).
- SDD process time of 4, to yield an optimum compromise between precision in the measurement of x-ray energies by the SDD detector and x-ray output count rates.
- Conditions chosen to yield dead times of ~50-60%, to maximize the x-ray output count rates in the EDS detector.
- Live acquisition times of 15 s.
- Pulse pileup and ZAF corrections applied during quantification using the Oxford software AZtec.
- Quantification using factory standard measurements, with frequent (daily to weekly) beam optimization performed on Cu tape; energy optimization – also using Cu tape – was performed following filament replacement.

- Si, Al, Ti, Fe, Mg, Mn, Ca, Na, and K quantified from the collected spectra; oxygen calculated by stoichiometry.
- Final results presented in oxide weight percentages, normalized to 100% anhydrous.

Additionally, for STM-1 and QLO-1, we performed analyses using live times of 30, 60, and 90 s, to test the effects of Na migration as a function of analytical time.

We collect populations of 15-30 individual analyses in succession for a given area of glass that is initially assumed to be homogeneous in composition. We calculate the average and standard deviation of each population to yield the best estimate of the glass composition and the uncertainty associated with these values. Consideration of the results allows testing of the initial assumption of homogeneity, and subpopulations can be defined when necessary. The standard deviation we calculate for each population is a measure of the repeatability measurement precision (i.e., the variability arising from multiple measurements on the same sample in the same analytical session, expressed as 1 standard deviation)(JCGM 200 2012), and it includes the effects of both analytical uncertainty and compositional variability of the fused glass.

We identify and remove outlier values of individual oxides using the median and interquartile range (IQR). Values outside the window of the median +/- 1.5*IQR are automatically excluded from the average and standard deviation calculations. In our studies of natural samples (see, for instance Pamukçu et al. 2021), we completely exclude individual analyses with four or more values identified as outliers (i.e., all oxides are excluded from the average and standard

deviation calculation). However, given the absence of crystals or vesicles in the fused glasses, no analyses were excluded in the present study.

For the sessions in which we tested longer analytical times (15-90 s), we calculate mean standard weighted deviation (MSWD) values (Wendt and Carl 1991) to characterize the extent of dispersion observed within each population relative to the analytical uncertainties. We use these values to assess the extent of Na migration in these populations.

Datasets

One of the datasets we present here (hereafter, "Short-term dataset") consists of analyses of synthesized glasses STM-1, QLO-1, and RGM-1 obtained over 12 analytical sessions that took place over 2 months (October-November 2023), with 1-2 populations of data collected for each of the reference materials in each session (no RGM-1 analyses for the first two sessions). This allows us to evaluate the quality of the data generated using the SEM-EDS at EES-Vanderbilt for a range of compositions relevant for silicic and alkaline magmas.

We also present a compilation of a large quantity of data for RGM-1 collected over the last 10 years (hereafter, "Long-term RGM dataset") using the SEM-EDS at EES-Vanderbilt (Pamukçu et al. 2020; Smithies et al. 2023; Chiaro et al. 2024; Harmon et al. 2024a, 2024b). This allows us to assess the long-term reproducibility of data generated using our instrument.

Data presented in the paper are available as a supplementary file available online.

Results

Short-term dataset

For live times of 15 s, the Short-term dataset includes 10 populations of RGM-1 glass (from analytical sessions 3-12), 13 populations of QLO-1 glass (two from session 11), and 12 populations of STM-1 (one from each session), as illustrated in Figure 2, Figure 3, and Table 1. As explained above, we report average compositions calculated from 15-30 individual spot analyses collected during each session. The dataset also includes populations for live times of 30, 60, and 90 s for QLO-1 (session 2) and STM-1 (session 1), as shown in Figure 4.

Visual inspection of our results for live times of 15 s suggests excellent reproducibility for both STM-1 and RGM-1 (see Figure 2 and Figure 3), and also excellent agreement with the reference values for the respective whole-rock reference materials (shown as squares in Figure 2 and Figure 3). Variations in values of abundant oxides such as SiO_2 and CaO are very small, and they show excellent accuracy (as measured by the ratio of measured to expected values), particularly for RGM-1 (ranging from 99.6% to 100.0% for SiO_2 and 100.7%-106.0% for CaO) and STM-1 (100.0%-100.3% for SiO_2 and 101.3%-105.6% for CaO), with QLO-1 showing inferior accuracy (100.0%-100.9% for SiO_2 and 91.9%-98.0% for CaO). Variations in K_2O are larger, but accuracy is excellent: 98.9%-100.3% for RGM-1, 97.7%-99.6% for STM-1, and 94.9%-101.0% for QLO-1. Results for Na_2O show slightly inferior accuracy, but are still very good: 95.5%-99.8% for RGM-1, 97.0%-99.9% for STM-1, and 96.7%-105.1% for QLO-1. Uncertainties are significantly larger for oxides in lower abundances (e.g., TiO_2, MnO), but reproducibility and agreement with reference values are still observed. The QLO-1 results show much greater variability; given that

these measurements were performed in the same analytical sessions as the measurements for STM-1 and RGM-1, and the range of values measured are similar, we infer that the variability in QLO-1 results is due to heterogeneity in the fused glass.

Results obtained for STM-1 and QLO-1 using longer live times show much larger variation (Figure 4), increasingly so with increasing live time (i.e., variability is largest for 90 s, and it decreases progressively to 60, 30, and 15 s). For live times greater than 15 s, values for Na_2O are systematically lower than expected, while values for other abundant oxides (e.g., SiO_2, K_2O) are systematically higher than expected. MSWD values for Na_2O concentrations are below 1 (and below the expected maximum MSWD threshold; see Table 2) for acquisition times of 15 s, and they increase rapidly, particularly for STM-1, with increasing acquisition time (Table 2). This suggests that the dispersion observed for data obtained with acquisition times of 15 s is well explained by the analytical uncertainties; in contrast, for acquisition times of 30, 60, and 90 s, the populations are overdispersed (i.e., observed MSWD is larger than the upper MSWD threshold), suggesting that the spread of data within each population is larger than what can be explained by the analytical uncertainties. This suggests that data obtained with 15 s acquisition time avoids significant Na migration.

Relative standard errors (i.e., standard deviation divided by concentration) for each oxide correlate strongly with concentration (Figure 2, Figure 3, and Figure 7). For oxides with concentrations >10 wt.%, relative standard errors are generally <1%; for concentrations between 1 and 10 wt.%, relative standard errors are typically <10%; for concentrations <1 wt.%, errors are much larger, and they can surpass 100% relative for concentrations of 0.1 wt.% or less.

Long-term RGM dataset

Results for RGM-1 obtained at EES-Vanderbilt since 2014 show excellent reproducibility over time (Figure 5, Figure 6), with uncertainties similar to those observed in the Short-term dataset (see Figure 2, Figure 3). We do not identify any trends over time.

Discussion

Quality of SEM-EDS analysis of natural silicate glasses

Our results show several important features of SEM-EDS analyses of natural silicate glasses:

1. Glass damage by the electron beam – and resulting migration of Na away from the beam – can be avoided by use of acquisition times of ≤15 s on our instrument under the conditions used.
2. Measured compositions are in excellent agreement with expected values, given the uncertainties estimated by repeated analysis of RGM-1 and STM-1 glasses within a session; QLO-1 glass shows heterogeneity that can be explained by insufficient homogenization during glass synthesis.
3. Precision obtained is excellent for major elements and adequate for minor elements, with oxides in concentrations ≤0.05 wt.% having uncertainties large enough that quantification is impractical.

These results are not surprising, in light of prior evidence suggesting that EDS analysis using SDD is superior to EDS analysis using older technology (Ritchie et al. 2012). Further, our results show that – for materials that are generally expected to be homogenous, such as volcanic glass

in pumice – repeated analysis of the material in a single session can yield appropriate estimates of uncertainty (specifically, estimates of intermediate precision) that include the effect of inhomogeneity of the analyzed material, in addition to counting statistics. This can not only lead to results that are more precise and accurate than those obtained using single spot analysis, but it also allows recognition of subtle differences and multiple compositional groups, as well as identification of materials that have suffered compositional changes due to alteration and weathering. Obtaining a larger number of analyses per sample results in much superior ability to assess compositional variability of volcanic glasses, which is more easily attainable with the shorter analytical times of SEM-EDS analyses (~15 s live time, ~30 s total) and lower operating costs compared with EMP-WDS analyses.

Comparison with EMP-WDS

In order to compare the quality of the SEM-EDS analyses obtained here with typical analysis by EMP-WDS, we compare the relationship between concentration and relative standard error we obtained for the Short-term dataset with the results of Loewen et al. (2023), obtained for a suite of glass reference materials used by the Alaska Volcano Observatory of the U.S. Geological Survey (AVO-USGS), as shown in Figure 7 (hereafter, "AVO dataset"). The advantage of this representation of the data is that it allows comparison of the precision achieved by the SEM-EDS and EMP-WDS, even though the specific glasses analyzed differ between the two laboratories.

For both datasets, we observe an approximately linear relationship in log-log space, suggesting a power-law relationship between concentration and relative standard error. Further, it is

striking that the SEM-EDS results show a steeper slope than the EMP-WDS results. This indicates that the precision obtained with SEM-EDS is potentially superior to that obtained using EMP-WDS for major elements in oxide concentrations greater than ~1 wt.%. For oxides in concentrations between ~0.5 and 1 wt.%, the two techniques yield results of similar precision. Finally, for minor elements with oxide concentrations lower than 0.5 wt.%, precision obtained with EMP-WDS is superior to that obtained with SEM-EDS.

These comparisons reveal that SEM-EDS is potentially preferable for analysis of major elements in natural silicate glasses. This can be explained by the combination of lower incident beam currents, use of a scanning beam, shorter acquisition times, better x-ray collection efficiency of the SDD detector compared to WDS detectors, and the lack of geometrical errors imposed by acquisition of data using a single detector in SEM-EDS analysis. It is useful to note that SEM-EDS analysis is performed using factory-supplied measurements of calibration materials (i.e., "standard-less"), which means that no calibration is necessary prior to analysis, rendering glass analysis by SEM-EDS much simpler and faster than analysis by EMP-WDS. Quality control of SEM-EDS analyses is performed by obtaining data for a secondary standard at the beginning of each analytical session, indicating that the instrument is performing adequately prior to analysis of any unknowns.

In contrast, EMP-WDS is preferable for analysis using electron-beam techniques of natural silicate glasses for minor elements, present in oxide abundances lower than ~0.5 wt.% and, particularly, for elements in oxide concentrations below 0.1 wt.% (Reed and Ware 1973). This is justified by the higher beam currents used (e.g., yielding higher counts), longer acquisition times, use of dedicated WDS detectors with much higher spectral resolution, and the small

effect of errors due to geometrical and beam-damage (i.e., Na-migration) on absolute oxide abundances measured (Reed 2005). Importantly, results obtained for major elements using EMP-WDS show very good precision, adequate for most applications.

One disadvantage of SEM-EDS analysis is that the total sum of oxides is not available, thus calculation of H_2O concentration by difference is typically not possible (at least in the case of "standard-less" analysis; see Geshi et al. 2021); it has been amply demonstrated that errors associated with such estimations are very large (unless specific correction methods are used; see Devine et al. 1995; Roman et al. 2006). Therefore, direct analysis of H_2O concentrations in silicate glasses by other methods is much preferred.

Implications

In this work, we show that both SEM-EDS and EMP-WDS can be successfully used for analysis of natural silicate glasses. For applications in which precision of major-element concentrations is paramount (e.g., glass geobarometry; see Gualda and Ghiorso 2014), SEM-EDS analysis is an excellent choice, possibly preferable to EMP-WDS. In contrast, for applications in which precision of minor elements is critical (e.g., Ti-in-quartz geochronometry; see Wark et al. 2007), use of EMP-WDS is preferred. For most applications, however, results obtained with both techniques are probably equally suitable. The much more widespread availability and lower usage costs of SEM-EDS systems stand as advantages when compared to EMP-WDS. Future work could explore the effectiveness of SEM-EDS analysis of minerals, in which spatial variability is expected, and effects of beam damage are much less severe or nonexistent.

Acknowledgements

We thank Jordan Lubbers and Matt Lowen for discussions that ultimately led to the idea of this manuscript. Reviews by Nicholas Ritchie and Jordan Lubbers and editorial handling by Paul Tomascak are greatly appreciated. Material support was provided by the National Science Foundation through grants EAR-0948528, EAR-0911726, EAR-1151337, and EAR-1830122 awarded to Gualda and by Vanderbilt University through internal funds. Any use of trade, firm, or product names is for descriptive purposes only and does not imply endorsement by the U.S. Government.

Data availability

All data used in the manuscript is presented within the manuscript, or in previous publications, as cited.

References

Abbey, S. (1983) Studies in "standard samples" of silicate rocks and minerals 1969-1982. Canadian Geological Survey Paper, 83–15, 114 p.

Chiaro, G.R., Gualda, G.A.R., Miller, C., Giordano, G., and Morelli, C. (2024) Mush Architecture and Processes in the Reservoirs of a Supereruption-Scale Magma System, Permian Ora Ignimbrite (Northern Italy). Journal of Petrology, 65, egae016.

Devine, J.D., Gardner, J.E., Brack, H.P., Layne, G.D., and Rutherford, M.J. (1995) Comparison of microanalytical methods for estimating H_2O contents of silicic volcanic glasses. American Mineralogist, 80, 319–328.

Flanagan, F.J. (1976) Descriptions and analyses of eight new USGS rock standards. U.S. Geological Survey Professional Paper, 840, 192 p.

Geshi, N., Yamasaki, T., Miyagi, I., and Conway, C.E. (2021) Magma chamber decompression during explosive caldera-forming eruption of Aira caldera. Communications Earth & Environment, 2, 200.

Gladney, E.S., and Roelandts, I. (1988) 1987 compilation of elemental concentration data for USGS BHVO-1, MAG-1, QLO-1, RGM-1, SCo-1, SDC-1, SGR-1, and STM-1. Geostandards Newsletter, 12, 253–362.

Govindaraju, K. (1994) 1994 compilation of working values and descriptions for 383 geostandards. Geostandards Newsletter, 18, 1–158.

Gualda, G.A.R., and Ghiorso, M.S. (2014) Phase-equilibrium geobarometers for silicic rocks based on rhyolite-MELTS. Part 1: Principles, procedures, and evaluation of the method. Contributions to Mineralogy and Petrology, 168, 1033.

Gualda, G.A.R., Grayley, D.M., Connor, M., Hollmann, B., Pamukçu, A.S., Begue, F., Ghiorso, M.S., and Deering, C.D. (2018) Climbing the crustal ladder: Magma storage-depth evolution during a volcanic flare-up. Science Advances, 4, eaap7567.

Gualda, G.A.R., Ghiorso, M.S., Hurst, A.A., Allen, M.C., and Bradshaw, R.W. (2022) A complex patchwork of magma bodies that fed the Bishop Tuff supereruption (Long Valley Caldera, CA, United States): Evidence from matrix glass major and trace-element compositions. Frontiers in Earth Science, 10, 798387.

Harmon, L.J., Gualda, G.A.R., Gravley, D.M., Smithies, S.L., and Deering, C.D. (2024a) The Whakamaru magmatic system (Taupō Volcanic Zone, New Zealand), part 1: Evidence from tephra deposits for the eruption of multiple magma types through time. Journal of Volcanology and Geothermal Research, 445, 107966.

Harmon, L.J., Smithies, S.L., Gualda, G.A.R., and Gravley, D.M. (2024b) The Whakamaru magmatic system (Taupō Volcanic Zone, New Zealand), part 2: Evidence from ignimbrite deposits for the pre-eruptive distribution of melt-dominated magma and magma mush. Journal of Volcanology and Geothermal Research, 447, 108013.

JCGM 200 (2012) International Vocabulary of Metrology – Basic and general concepts and associated terms (VIM), 3rd edition.

Loewen, M.W., Wallace, K.L., Lubbers, J., Ruth, D., Izbekov, P.E., Larsen, J.F., and Graham, N. (2023) Glass electron microprobe analyses methods, precision and accuracy for tephra studies in Alaska. Alaska Division of Geological & Geophysical Surveys Miscellaneous Publication, 174, 20 p.

Morgan, G.B., and London, D. (2005) Effect of current density on the electron microprobe analysis of alkali aluminosilicate glasses. American Mineralogist, 90, 1131–1138.

Newbury, D.E., and Ritchie, N.W.M. (2015) Performing elemental microanalysis with high accuracy and high precision by scanning electron microscopy/silicon drift detector energy-dispersive X-ray spectrometry (SEM/SDD-EDS). Journal of Materials Science, 50, 493–518.

Pamukçu, A.S., Wright, K.A., Gualda, G.A.R., and Gravley, D. (2020) Magma residence and eruption at the Taupo Volcanic Center (Taupo Volcanic Zone, New Zealand): insights from rhyolite-MELTS geobarometry, diffusion chronometry, and crystal textures. Contributions to Mineralogy and Petrology, 175, 48.

Pamukçu, A.S., Gualda, G.A.R., and Gravley, D.M. (2021) Rhyolite-MELTS and the storage and extraction of large-volume crystal-poor rhyolitic melts at the Taupō Volcanic Center: a reply to Wilson et al. (2021). Contributions to Mineralogy and Petrology, 176, 82.

Pitcher, B.W., Gualda, G.A.R., and Hasegawa, T. (2021) Repetitive Duality of Rhyolite Compositions, Timescales, and Storage and Extraction Conditions for Pleistocene Caldera-forming Eruptions, Hokkaido, Japan. Journal of Petrology, 62, egaa106.

Potts, P.J. (1987) A handbook of silicate rock analysis, 622 p. Chapman and Hall, New York.

Reed, S.J.B. (2005) Electron Microprobe Analysis and Scanning Electron Microscopy in Geology, 2nd ed. Cambridge University Press.

Reed, S.J.B., and Ware, N.G. (1973) Quantitative electron microprobe analysis using a lithium drifted silicon detector. X-Ray Spectrometry, 2, 69–74.

Ritchie, N.W.M., Newbury, D.E., and Davis, J.M. (2012) EDS Measurements of X-Ray Intensity at WDS Precision and Accuracy Using a Silicon Drift Detector. Microscopy and Microanalysis, 18, 892–904.

Roman, D.C., Cashman, K.V., Gardner, C.A., Wallace, P.J., and Donovan, J.J. (2006) Storage and interaction of compositionally heterogeneous magmas from the 1986 eruption of Augustine Volcano, Alaska. Bulletin of Volcanology, 68, 240–254.

Smithies, S.L., Harmon, L.J., Allen, S.M., Gravley, D.M., and Gualda, G.A.R. (2023) Following magma: The pathway of silicic magmas from extraction to storage during an ignimbrite flare-up, Taupō Volcanic Zone, New Zealand. Earth and Planetary Science Letters, 607, 118053.

Wark, D.A., Hildreth, W., Spear, F.S., Cherniak, D.J., and Watson, E.B. (2007) Pre-eruption recharge of the Bishop magma system. Geology, 35, 235–238.

Wendt, I., and Carl, C. (1991) The statistical distribution of the mean squared weighted deviation. Chemical Geology: Isotope Geoscience section, 86, 275–285.

Figure captions

Figure 1. Example of backscattered electron (BSE) image showing analyzed areas for quantitative analysis of the RGM-1 standard using the SEM-EDS at the Department of Earth & Environmental Sciences, Vanderbilt University.

Figure 2. Binary diagrams showing results of analysis of reference materials STM-1, QLO-1, and RGM-1 by SEM-EDS (small colored symbols), compared with expected values (large colored squares). Average compositions of ~10-15 spot analyses collected during each analytical session are shown as separate symbols, with uncertainties (i.e., the repeatability measurement precision, expressed as 1 standard deviation) shown by black error bars. Results for STM-1 and RGM-1 reproduce the expected values very well, with uncertainties increasing with decreasing oxide abundance. For QLO-1, significant variability is observed, suggesting heterogeneity in the fused glass.

Figure 3. Diagrams showing results of analysis of reference materials STM-1, QLO-1, and RGM-1 by SEM-EDS (small colored symbols) as a function of analytical session, compared with expected values (large colored squares at session 0). Each small symbol represents the average composition of ~10-15 spot analyses, with uncertainties (i.e., the repeatability measurement precision, expressed as 1 standard deviation) indicated by black error bars. No trends over time are seen, and results for STM-1 and RGM-1 show good agreement between our results and expected values. For QLO-1, results for CaO, K_2O and FeO show much larger variability, with some values falling outside what would be expected based on the reference values, suggesting heterogeneity in the fused glass.

Figure 4. Binary diagrams showing the relationship between SiO_2 and Na_2O for individual analyses using a wider range of analytical times for STM-1 and QLO-1. On the top diagrams, individual analyses are shown as separate symbols, showing the range of results obtained for each analytical time used. On the bottom diagram, the mean value for each analytical time is shown, with error bars representing 1 standard deviation. Diagrams on the left show results for STM-1, while diagrams on the right show results for QLO-1. For analytical times of 15 s (circles), there is no significant trend in the diagram, showing that no significant Na loss takes place. For times of 30 s (diamonds), 60 s (triangles), and 90 s (squares), there is a strong negative correlation between SiO_2 and Na_2O, showing Na migration from the analyzed area, and corresponding increase in SiO_2. The longer the time, the larger the effect. For STM-1, in which Na_2O concentrations are much higher than in QLO-1, the observed effect is also larger.

Figure 5. Binary diagrams showing results of analysis of reference material RGM-1 obtained using the EES-Vanderbilt SEM-EDS since 2014 (labeled according to each study), compared with expected values (gray squares with error bars). Results show excellent reproducibility, as well as excellent agreement between our measurements and expected values.

Figure 6. Diagrams showing results of analysis of reference material RGM-1 by SEM-EDS (small colored symbols) as a function of analytical session (ordered as a function of time, labeled according to each study), compared with expected values (large gray squares, off scale to the left of session 0). Agreement with expected values is excellent, and there are no evident trends over time, showing the reliability of analysis of silicic glasses by SEM-EDS. Notice that, for some of the data, MnO values were not quantified, and they are plotted at 0 concentration.

Figure 7. Log-log diagram showing the relationship between concentration and relative standard error (two standard deviations – i.e., 2-sigma – divided by concentration). Colored symbols show our results for reference materials STM-1, QLO-1, and RGM-1 (labeled Vanderbilt dataset; see text for details), while gray dots represent data from Loewen et al. (2023) for a large suite of reference materials (AVO dataset; see text for details). Uncertainties obtained by both methods are similar, but SEM-EDS results show smaller uncertainties for concentrations >1 wt.%, while EMP-WDS results show smaller uncertainties for concentrations <0.5 wt.%.

Tables

Table 1. Expected values and associated uncertainties for reference materials STM-1, QLO-1, and RGM-1.

	STM-1		**QLO-1**		**RGM-1**	
	Expected	*Uncertainty*	*Expected*	*Uncertainty*	*Expected*	*Uncertainty*
SiO_2	61.15	0.50	66.68	0.48	74.23	0.54
TiO_2	0.14	0.01	0.63	0.03	0.27	0.02
Al_2O_3	18.88	0.24	16.46	0.19	13.86	0.19
MgO	0.10	0.02	1.02	0.07	0.28	0.03
FeO	4.82	0.09	3.96	0.09	1.69	0.03
MnO	0.23	0.02	0.09	0.01	0.04	0.00
CaO	1.12	0.06	3.22	0.08	1.16	0.07
Na_2O	9.17	0.21	4.27	0.13	4.12	0.15
K_2O	4.39	0.07	3.66	0.12	4.35	0.10

Table 2. MSWD values for populations of data for reference materials STM-1 and QLO-1 obtained with different acquisition times (15, 30, 60, and 90 s).

Population	**MSWD**	**n**	**MSWD upper threshold**
STM-1 15 s	0.83	20	1.65
STM-1 30 s	3.65	20	1.65
STM-1 60 s	35.0	20	1.65
STM-1 90 s	175	20	1.65
QLO-1 15 s	0.44	20	1.65
QLO-1 15 s (2)	0.67	20	1.65
QLO-1 30 s	1.18	12	1.85
QLO-1 60 s	11.8	5	2.41
QLO-1 90 s	9.60	20	1.65

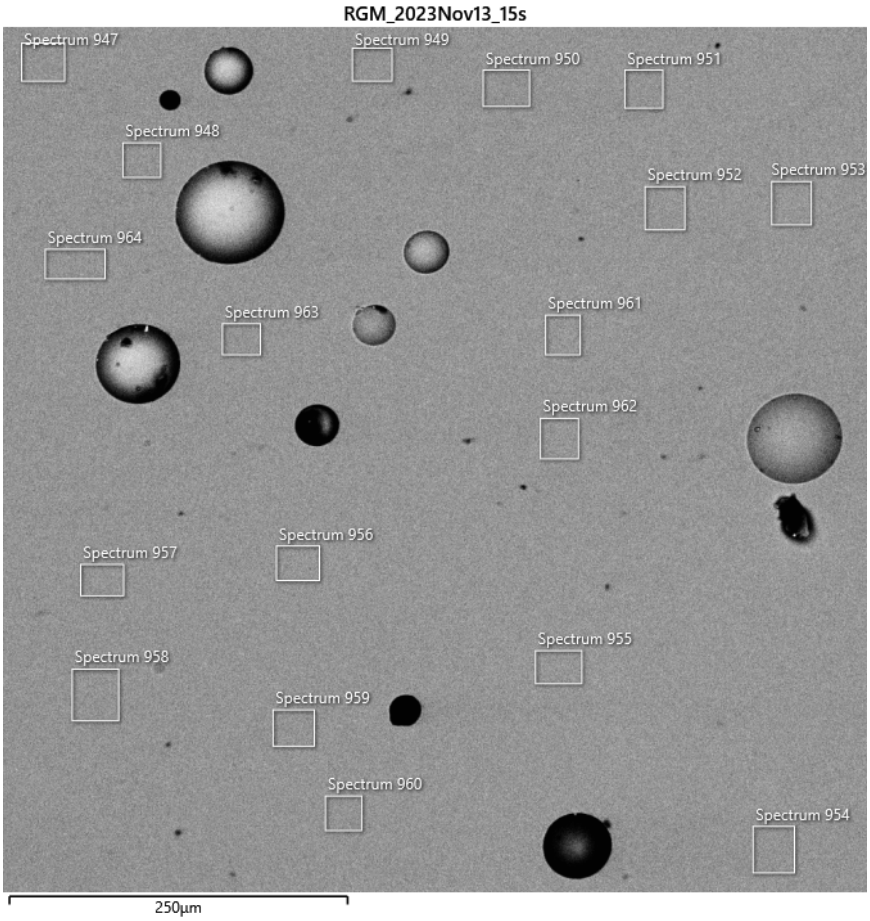
RGM_2023Nov13_15s
Spectrum 947
Spectrum 949
Spectrum 950
Spectrum 951
Spectrum 948
Spectrum 952
Spectrum 953
Spectrum 964
Spectrum 963
Spectrum 961
Spectrum 962
Spectrum 956
Spectrum 957
Spectrum 955
Spectrum 958
Spectrum 959
Spectrum 960
Spectrum 954
250µm

Figure 1

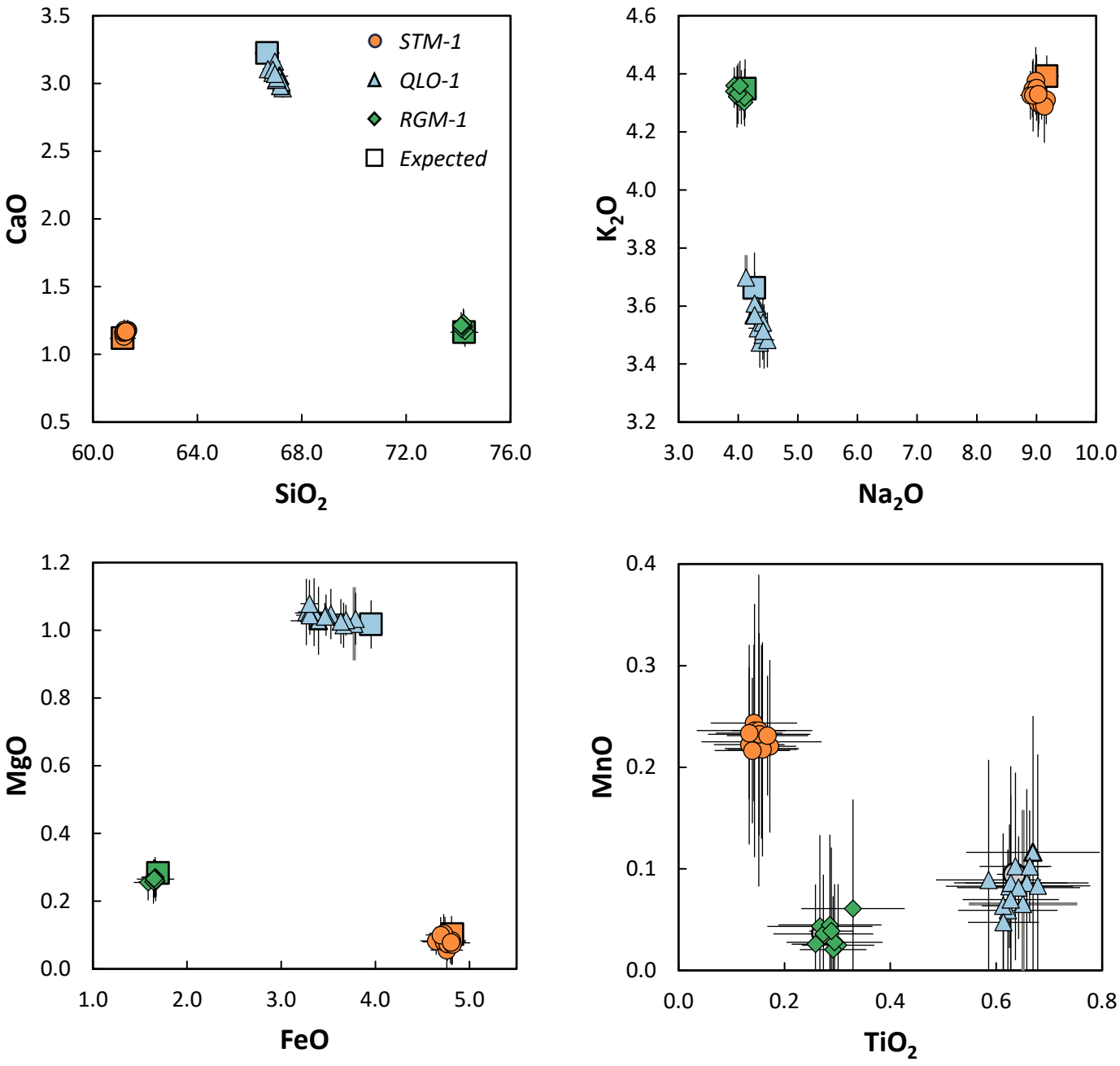

Figure 2

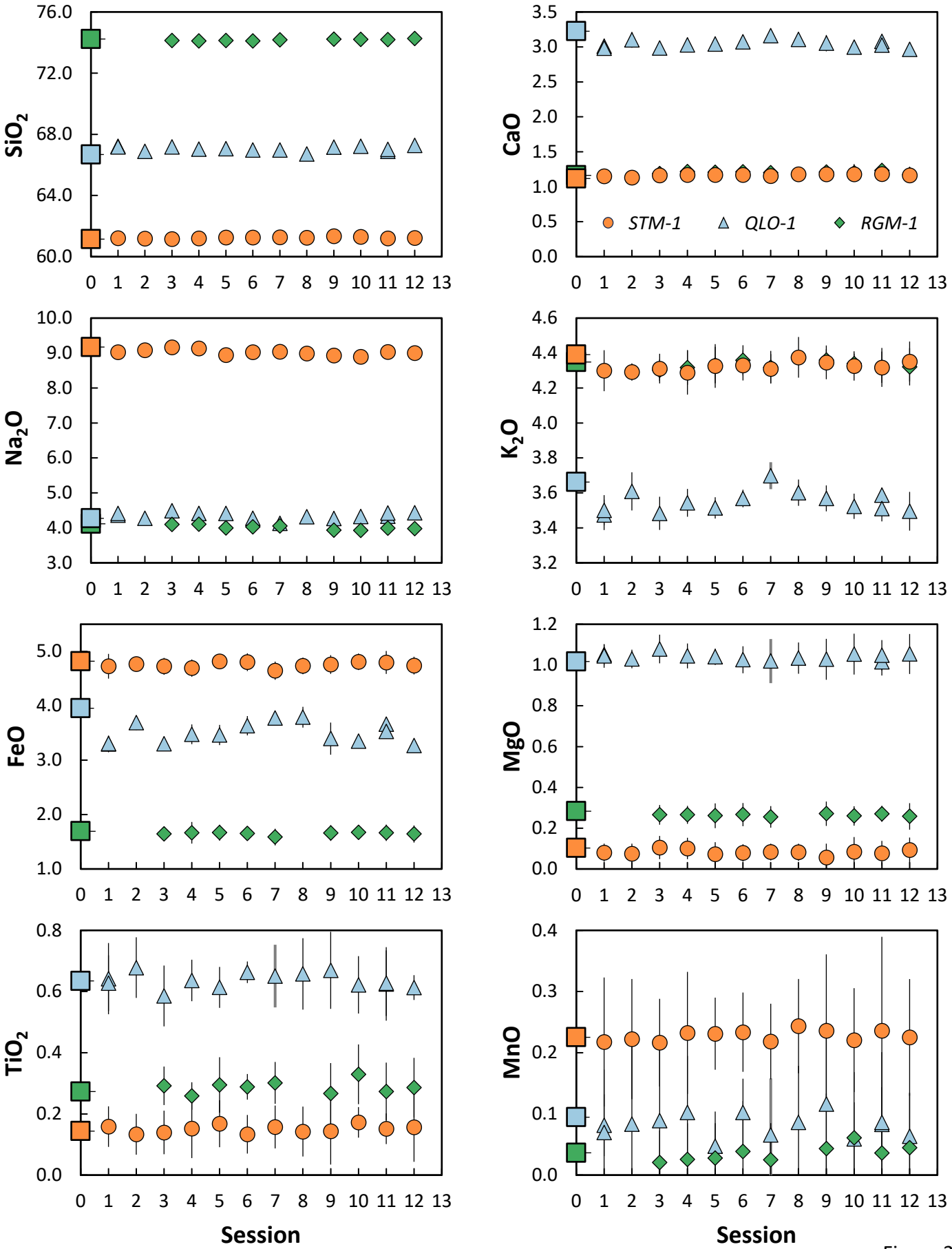
SiO2
CaO
Na2O
K2O
FeO
MgO
TiO2
MnO
STM-1
QLO-1
RGM-1
Session
Session

Figure 3

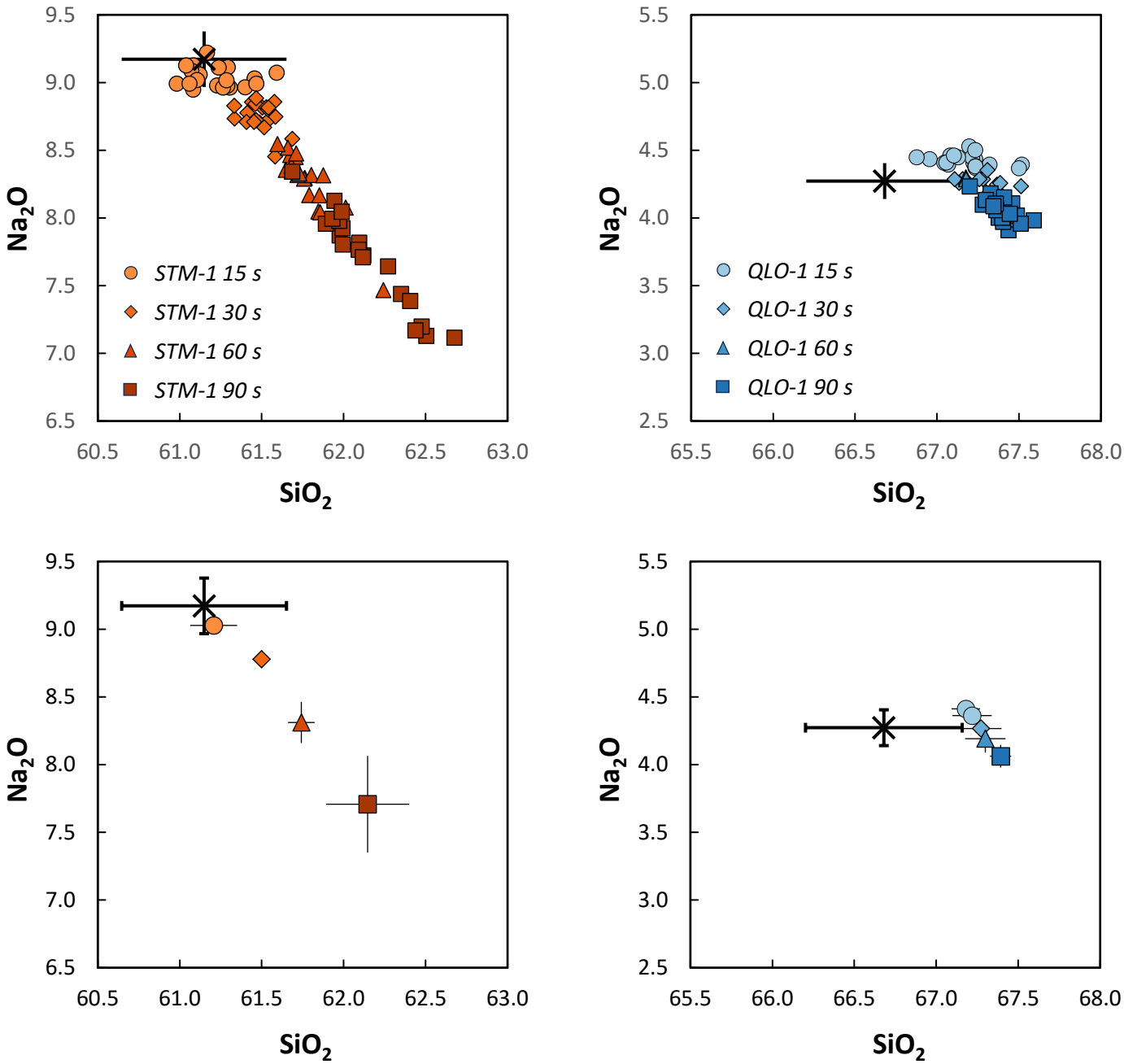
9.5
9.0
8.5
8.0
7.5
7.0
6.5
Na_2O
STM-1 15 s
STM-1 30 s
STM-1 60 s
STM-1 90 s
60.5
61.0
61.5
62.0
62.5
63.0
SiO_2
5.5
5.0
4.5
4.0
3.5
3.0
2.5
Na_2O
QLO-1 15 s
QLO-1 30 s
QLO-1 60 s
QLO-1 90 s
65.5
66.0
66.5
67.0
67.5
68.0
SiO_2
9.5
9.0
8.5
8.0
7.5
7.0
6.5
Na_2O
60.5
61.0
61.5
62.0
62.5
63.0
SiO_2
5.5
5.0
4.5
4.0
3.5
3.0
2.5
Na_2O
65.5
66.0
66.5
67.0
67.5
68.0
SiO_2

Figure 4

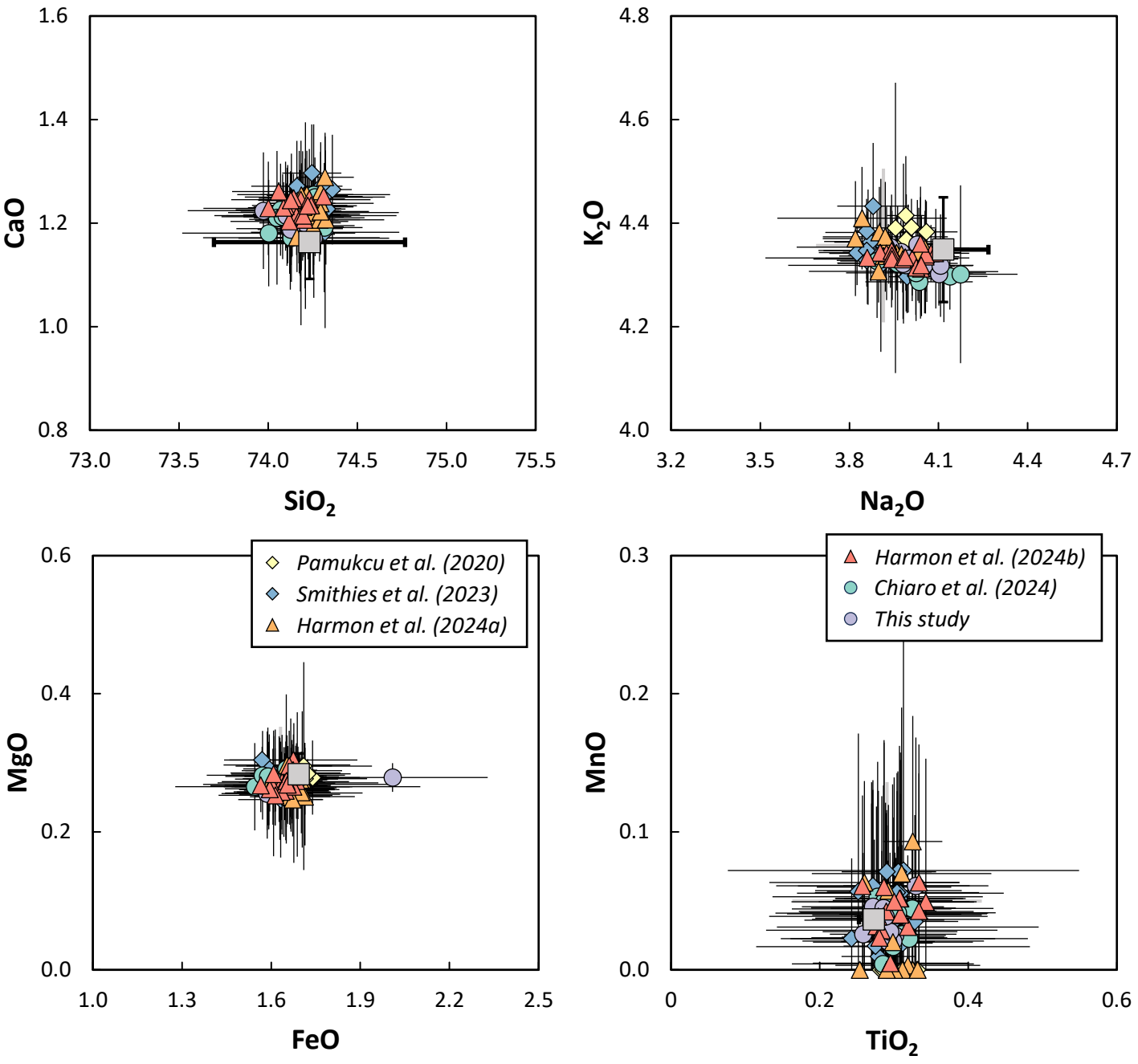
1.6
1.4
1.2
1.0
0.8
CaO
73.0
73.5
74.0
74.5
75.0
75.5
SiO2
4.8
4.6
4.4
4.2
4.0
K2O
3.2
3.5
3.8
4.1
4.4
4.7
Na2O
0.6
0.4
0.2
0.0
MgO
1.0
1.3
1.6
1.9
2.2
2.5
FeO
Pamukcu et al. (2020)
Smithies et al. (2023)
Harmon et al. (2024a)
0.3
0.2
0.1
0.0
MnO
0
0.2
0.4
0.6
TiO2
Harmon et al. (2024b)
Chiaro et al. (2024)
This study

Figure 5

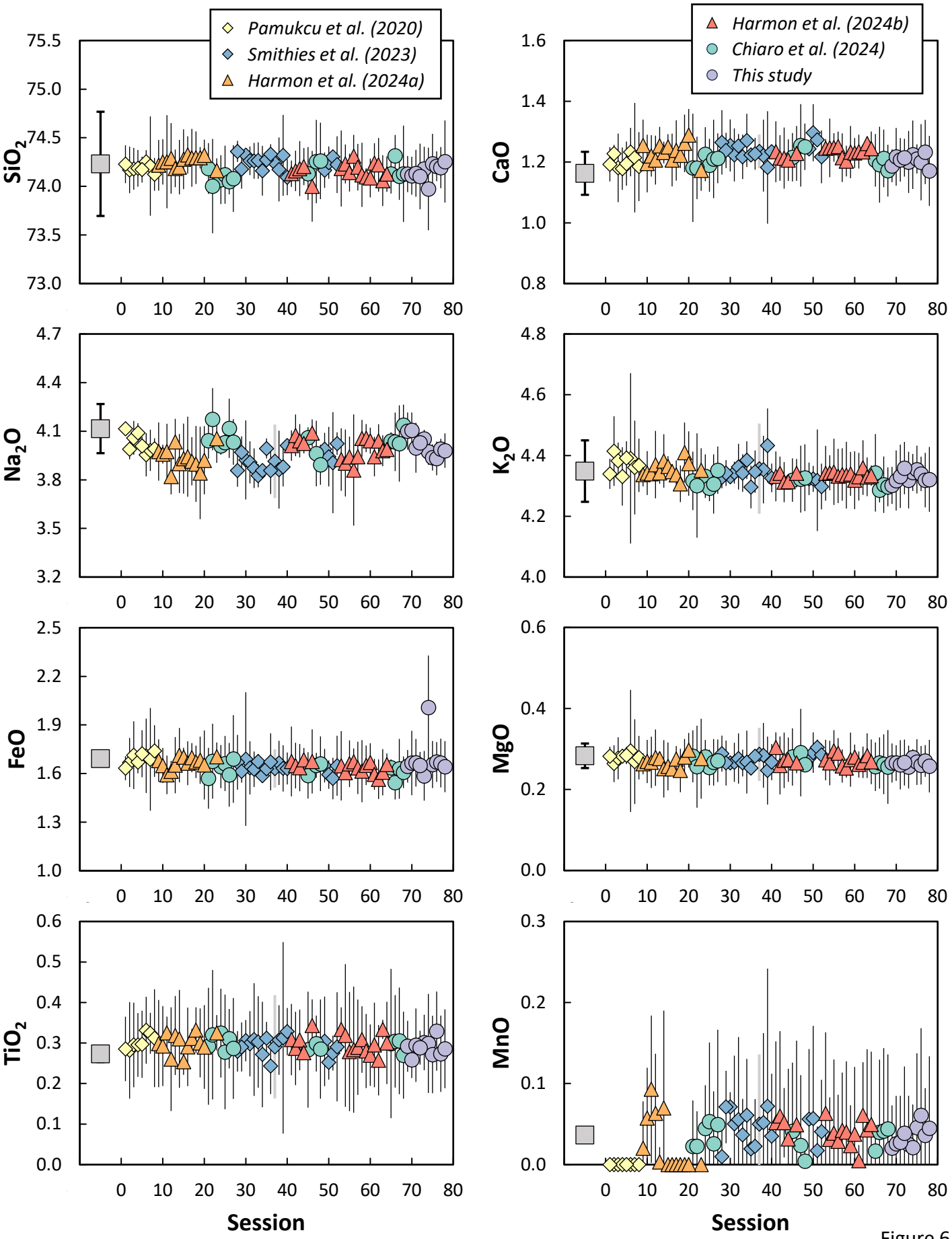
Pamukcu et al. (2020)
Smithies et al. (2023)
Harmon et al. (2024a)
Harmon et al. (2024b)
Chiaro et al. (2024)
This study
SiO2
CaO
Na2O
K2O
FeO
MgO
TiO2
MnO
Session
Session

Figure 6

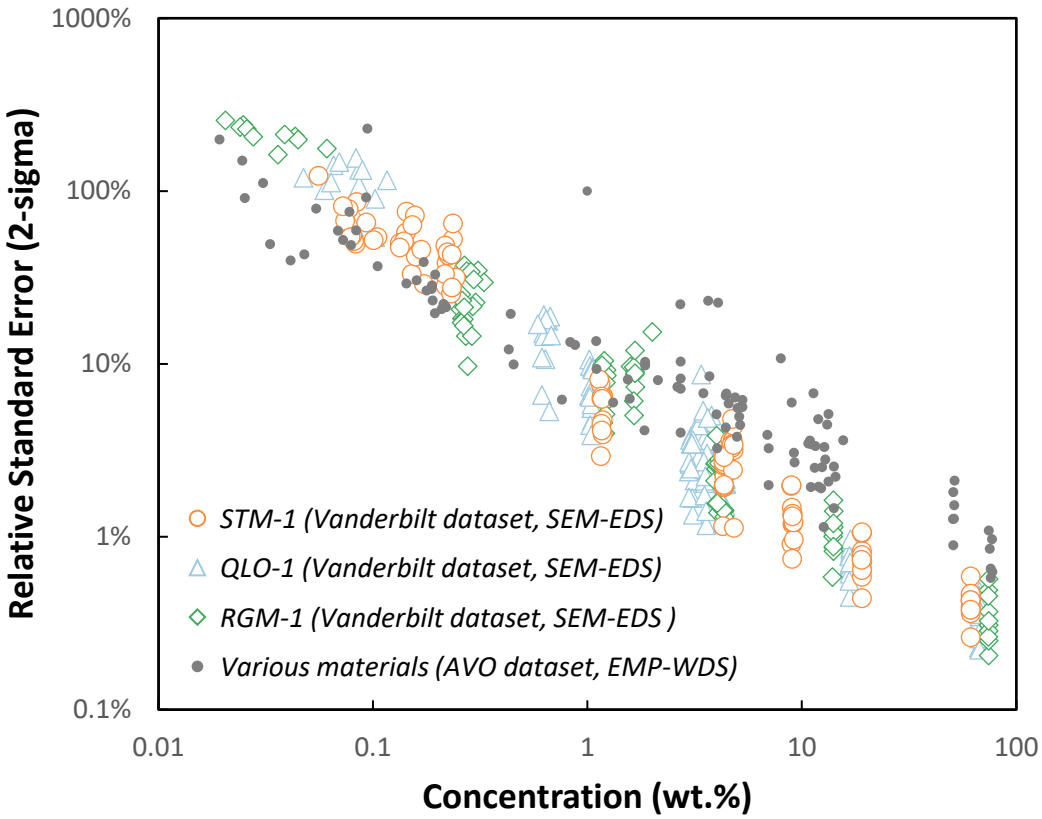
1000%
100%
10%
1%
0.1%
Relative Standard Error (2-sigma)
0.01
0.1
1
10
100
Concentration (wt.%)
STM-1 (Vanderbilt dataset, SEM-EDS)
QLO-1 (Vanderbilt dataset, SEM-EDS)
RGM-1 (Vanderbilt dataset, SEM-EDS)
Various materials (AVO dataset, EMP-WDS)

Figure 7